

# NaZn(H<sub>2</sub>O)<sub>2</sub>[BP<sub>2</sub>O<sub>8</sub>]·H<sub>2</sub>O: A Novel Open-Framework Borophosphate and its Reversible Dehydration to Microporous Sodium Zincoborophosphate Na[ZnBP<sub>2</sub>O<sub>8</sub>]·H<sub>2</sub>O with CZP Topology

Insan Boy,<sup>[b]</sup> Frank Stowasser,<sup>[c]</sup> Gerd Schäfer,<sup>[a]</sup> and Rüdiger Kniep\*<sup>[a]</sup>

**Abstract:** Crystals of NaZn(H<sub>2</sub>O)<sub>2</sub>[BP<sub>2</sub>O<sub>8</sub>]·H<sub>2</sub>O were grown under mild hydrothermal conditions at 170 °C. The crystal structure (solved by X-ray single-crystal methods: hexagonal, *P*6<sub>1</sub>22 (no. 178), *a* = 946.2(2), *c* = 1583.5(1) pm, *V* = 1227.8(4) · 10<sup>6</sup> pm<sup>3</sup>, *Z* = 6) exhibits a chiral octahedral-tetrahedral framework related to the CZP topology and contains helical ribbons of corner-linked borate and phosphate tetrahedra. Investigation of the thermal behavior up to

180 °C shows a (reversible) dehydration process; this leads to the microporous compound Na[ZnBP<sub>2</sub>O<sub>8</sub>]·H<sub>2</sub>O, which has the CZP topology. The crystal structure of Na[ZnBP<sub>2</sub>O<sub>8</sub>]·H<sub>2</sub>O was determined by X-ray powder diffraction by

using a combination of simulated annealing, lattice-energy minimization, and Rietveld refinement procedures (hexagonal, *P*6<sub>1</sub>22 (no. 178), *a* = 954.04(2), *c* = 1477.80(3) pm, *V* = 1164.88(5) · 10<sup>6</sup> pm<sup>3</sup>, *Z* = 6). The essential structural difference caused by the dehydration concerns the coordination of Zn<sup>2+</sup> changing from octahedral to tetrahedral arrangement.

**Keywords:** boron · microporosity · phosphates · reversible dehydration · solid-state structures · zeolite analogues

## Introduction

Our recent research on compounds with framework structures<sup>[1]</sup> is focussed on borophosphates (intermediate phases in systems M<sub>x</sub>O<sub>y</sub>-B<sub>2</sub>O<sub>3</sub>-P<sub>2</sub>O<sub>5</sub>-(H<sub>2</sub>O)).<sup>[2]</sup> Although systematic investigations on borophosphates have started only in the last few years,<sup>[3]</sup> a broad spectrum of new compounds has already been characterized with various anionic partial structures, such as oligomeric units,<sup>[4]</sup> chains,<sup>[3, 5]</sup> ribbons,<sup>[6]</sup> layers,<sup>[7]</sup> and three-dimensional frameworks.<sup>[8]</sup> Systematic treatments of the structural chemistry of borophosphates have also been approached.<sup>[2]</sup> In relation to microporous and zeolite-analogous systems such as aluminosilicates,<sup>[9]</sup> aluminium/alumophos-

phates,<sup>[10]</sup> substituted variants,<sup>[11]</sup> and gallium/gallo-<sup>[12]</sup> and zincophosphates,<sup>[13]</sup> we have succeeded in characterizing new open-framework structures based on boro- and zincoborophosphates. With the syntheses of A[ZnBP<sub>2</sub>O<sub>8</sub>] (A = K<sup>+</sup>, NH<sub>4</sub><sup>+</sup>, Rb<sup>+</sup>, Cs<sup>+</sup>) a new class of compounds with tetrahedral frameworks has been realized, whose topologies display a close relationship to aluminosilicates (feldspar family and gismondine).<sup>[14]</sup> A chiral octahedral-tetrahedral framework related to the CZP topology<sup>[15]</sup> is present in the crystal structures of compounds M<sup>I</sup>M<sup>II</sup>(H<sub>2</sub>O)<sub>2</sub>[BP<sub>2</sub>O<sub>8</sub>]·yH<sub>2</sub>O (M<sup>I</sup>: Li, Na, K; M<sup>II</sup>: Mn, Fe, Co, Ni, Zn; y: 0.5, 1),<sup>[2b, 6a]</sup> which contain helical ribbons of corner-linked borate and phosphate tetrahedra. Here, we report on the crystal structure of NaZn(H<sub>2</sub>O)<sub>2</sub>[BP<sub>2</sub>O<sub>8</sub>]·H<sub>2</sub>O, which shows a remarkable thermal behavior up to 180 °C. NaZn(H<sub>2</sub>O)<sub>2</sub>[BP<sub>2</sub>O<sub>8</sub>]·H<sub>2</sub>O reversibly releases (and reabsorbs) water, a process which is accompanied by a change of Zn<sup>II</sup> coordination as the essential structural consequence. The dehydrated compound (Na[ZnBP<sub>2</sub>O<sub>8</sub>]·H<sub>2</sub>O) is characterized by a microporous, chiral tetrahedral framework of CZP topology.

## Results and Discussion

**NaZn(H<sub>2</sub>O)<sub>2</sub>[BP<sub>2</sub>O<sub>8</sub>]·H<sub>2</sub>O:** The crystal structure of NaZn(H<sub>2</sub>O)<sub>2</sub>[BP<sub>2</sub>O<sub>8</sub>]·H<sub>2</sub>O reveals an infinite one-dimensional anionic partial structure. The condensation of BO<sub>4</sub> and PO<sub>4</sub> tetrahedra through common vertices leads to tetrahedral

[a] Prof. Dr. R. Kniep, Dipl.-Ing. G. Schäfer  
Max-Planck-Institut für Chemische Physik fester Stoffe  
Nöthnitzer Str. 40, 01187 Dresden (Germany)  
Fax: (+49) 351-4646-3002  
E-mail: kniep@cphys.mpg.de

[b] Dr. I. Boy  
Eduard-Zintl-Institut der Technischen Universität  
Hochschulstr. 10, 64289 Darmstadt (Germany)  
Fax: (+49) 6151-16-6029  
E-mail: boy@ac.chemie.tu-darmstadt.de

[c] Dipl.-Min. F. Stowasser  
Lehrstuhl für Anorganische Chemie II  
Ruhr-Universität-Bochum  
Universitätsstr. 150, 44780 Bochum (Germany)  
Fax: (+49) 234-32-14174  
E-mail: stowafbu@rz.ruhr-uni-bochum.de

ribbons of  $\infty\{[\text{BP}_2\text{O}_8]^{3-}\}$ , which are arranged around  $6_1$  screw axes to form helices (Figure 1). The helical ribbons are built up from four-membered rings of tetrahedra in which  $\text{BO}_4$  and

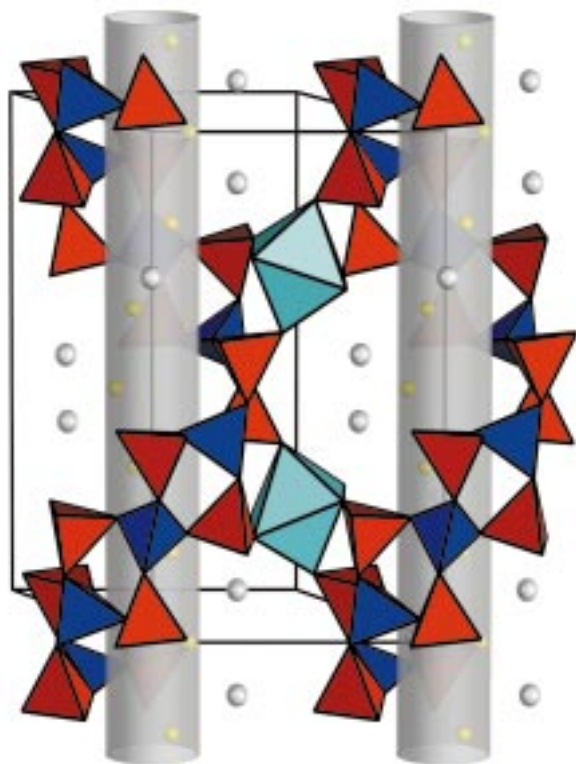


Figure 1. Linkage of borophosphate helices in the crystal structure of the hydrated phase  $\text{NaZn}(\text{H}_2\text{O})_2[\text{BP}_2\text{O}_8] \cdot \text{H}_2\text{O}$  through  $\text{ZnO}_4(\text{H}_2\text{O})_2$  octahedra ( $\text{BO}_4$  tetrahedra: blue,  $\text{PO}_4$  tetrahedra: red,  $\text{Na}^+$ : grey spheres,  $\text{H}_2\text{O}$  in the helical channels: yellow spheres,  $\text{Zn}^{\text{II}}$  octahedral: turquoise). For further details see text.

**Abstract in German:**  $\text{NaZn}(\text{H}_2\text{O})_2[\text{BP}_2\text{O}_8] \cdot \text{H}_2\text{O}$  wurde unter milden hydrothermalen Bedingungen bei  $170^\circ\text{C}$  dargestellt. Die Kristallstruktur (Einkristalldaten, hexagonal,  $P6_322$  (Nr. 178),  $a = 946.2(2)$ ,  $c = 1583.5(1)$  pm,  $V = 1227.8(4) \cdot 10^6$  pm<sup>3</sup>,  $Z = 6$ ) enthält einen makromolekularen Anionenverband aus eckverknüpften Borat- und Phosphat-Tetraedern, die sich um  $6_1$ -Schraubenachsen zu Helices anordnen. Die Verknüpfung der Anionenteilstruktur über gemeinsame Ecken mit  $\text{Zn}^{\text{II}}$ -Oktaedern führt zu einem dreidimensionalen Gerüst, dessen Topologie derjenigen des CZP-Typs nahe verwandt ist. Thermische Untersuchungen bis  $180^\circ\text{C}$  belegen einen (reversiblen) Dehydratisierungsprozess, der zur mikroporösen Verbindung  $\text{Na}[\text{ZnBP}_2\text{O}_8] \cdot \text{H}_2\text{O}$  mit CZP-Topologie führt. Die Kristallstruktur von  $\text{Na}[\text{ZnBP}_2\text{O}_8] \cdot \text{H}_2\text{O}$  wurde aus Röntgenpulverdaten über den kombinierten Einsatz von Methoden der Gitterenergie-Minimierung, Simulated Annealing und Rietveld-Verfeinerungen aufgeklärt (hexagonal,  $P6_322$  (Nr. 178),  $a = 954.04(2)$ ,  $c = 1477.80(3)$  pm,  $V = 1164.88(5) \cdot 10^6$  pm<sup>3</sup>,  $Z = 6$ ). Die durch den Dehydratisierungsprozess verursachte wesentliche strukturelle Änderung betrifft die Umgebung von  $\text{Zn}^{2+}$ , dessen Koordinationszahl von sechs (oktaderisch) auf vier (tetraedrisch) verringert wird.

$\text{PO}_4$  groups alternate. Each  $\text{BO}_4$  tetrahedron is joined to the adjacent four-membered rings of  $\text{PO}_4$  tetrahedra along the ribbon in such a way that all vertices of the  $\text{BO}_4$  groups participate in bridging functions with  $\text{PO}_4$  tetrahedra. The phosphate groups occupy the borders of the ribbons with two terminal oxygen atoms, which act as ligands to complete the coordination sphere around  $\text{Zn}^{2+}$ .

The free loops of the borophosphate helices are occupied by  $\text{Na}^+$ , which are fixed by an irregular arrangement of eight  $[6+2]$  oxygen atoms from adjacent phosphate groups ( $\text{O}_3$ ,  $\text{O}_5$ ) and water molecules ( $\text{O}_{2\text{H}_2\text{O}}$ ,  $\text{O}_{6\text{H}_2\text{O}}$ ). A double helix  $\infty\{\text{Na}[\text{BP}_2\text{O}_8]^{2-}\}$  is completed; it forms a central channel running along the  $6_1$  screw axis, which is filled with water molecules ( $\text{O}_{6\text{H}_2\text{O}}$ ) resulting in the formula  $\infty\{\text{Na}[\text{BP}_2\text{O}_8]^{2-} \cdot \text{H}_2\text{O}\}$ . The water molecules form hydrogen bonds ( $\text{O}_{6\text{H}_2\text{O}} \cdots \text{O}_{6\text{H}_2\text{O}} = 293$  pm) with each other along the helix. The  $\text{Zn}^{2+}$  ion is coordinated by the oxygen atoms of  $\text{PO}_4$  groups ( $\text{O}_3$ ,  $\text{O}_5$ ) and water molecules ( $\text{O}_{2\text{H}_2\text{O}}$ ); this results in octahedral coordination,  $\text{Zn}(\text{O}_p)_4(\text{O}_{\text{H}_2\text{O}})_2$ .

The remarkable organization of the crystal structure of  $\text{NaZn}(\text{H}_2\text{O})_2[\text{BP}_2\text{O}_8] \cdot \text{H}_2\text{O}$  can be recognized in a view along the  $c$  axis (Figure 2, left), which shows the arrangement in radial shells: central  $\text{O}_{6\text{H}_2\text{O}}$  helix (diameter  $\sim 254$  pm), B helix (diameter  $\sim 502$  pm), P helix (diameter  $\sim 640$  pm), Na helix (diameter  $\sim 633$  pm), followed by a helix of coordination water  $\text{O}_{2\text{H}_2\text{O}}$  (diameter  $\sim 809$  pm), and finally a Zn helix (diameter  $\sim 946$  pm).

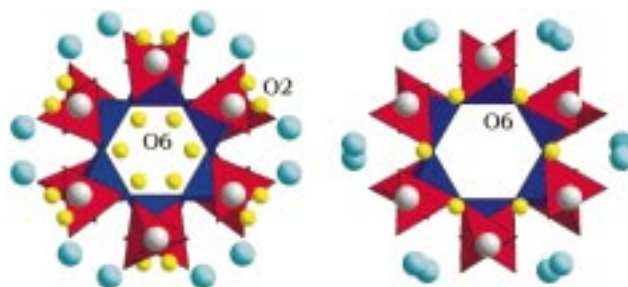


Figure 2. Sections of the crystal structure of the hydrated phase  $\text{NaZn}(\text{H}_2\text{O})_2[\text{BP}_2\text{O}_8] \cdot \text{H}_2\text{O}$  (left) and the dehydrated phase  $\text{Na}[\text{ZnBP}_2\text{O}_8] \cdot \text{H}_2\text{O}$  (right) as viewed along the hexagonal  $c$  axis ( $\text{BO}_4$  tetrahedra: blue,  $\text{PO}_4$  tetrahedra: red,  $\text{Na}^+$ : grey spheres,  $\text{H}_2\text{O}$ : yellow spheres,  $\text{Zn}^{2+}$ : turquoise spheres).

The helical tetrahedral ribbons are linked by  $\text{ZnO}_4(\text{H}_2\text{O})_2$  coordination octahedra, giving a chiral octahedral-tetrahedral framework related to the CZP topology (IZA structure designation CZP), which has been previously observed in the crystal structures of  $\text{NaZnPO}_4 \cdot \text{H}_2\text{O}$ <sup>[16]</sup> and its cobalt-substituted<sup>[17]</sup> variant (tetrahedral frameworks). In comparison to these crystal structures, boron in the title compound replaces the position of Zn1 in  $\text{NaZnPO}_4 \cdot \text{H}_2\text{O}$ .

**$\text{Na}[\text{ZnBP}_2\text{O}_8] \cdot \text{H}_2\text{O}$ :** The crystal structure of the dehydrated phase  $\text{Na}[\text{ZnBP}_2\text{O}_8] \cdot \text{H}_2\text{O}$  exhibits mainly differences in  $\text{Zn}^{2+}$  and  $\text{Na}^+$  coordination due to the release of  $\text{H}_2\text{O}$  ligands (coordination water  $\text{O}_{2\text{H}_2\text{O}}$  in the crystal structure of  $\text{NaZn}(\text{H}_2\text{O})_2[\text{BP}_2\text{O}_8] \cdot \text{H}_2\text{O}$ ). With respect to the hydrated phase the unit cell has a contraction in volume of 5%. This amount of

shrinkage is achieved from the reduction of the  $c$  lattice parameter by 7%, while the hexagonal basis is slightly enlarged (see Tables 1 and 4 in the Experimental Section).

The octahedral coordination of  $Zn^{2+}$  (hydrated phase) changes to tetrahedral environment (dehydrated phase) because of the release of the Zn-coordinating  $O_{2H_2O}$  (Figure 3). The coordination number of  $Na^+$  at the same time decreases from [6+2] to [6]. This change in coordination is only affected by minor translations of the remaining oxygen positions. Besides the loss of  $O_{2H_2O}$  the major structural change concerns the displacement of the water molecules  $O_{6H_2O}$ , which are shifted remarkably out of positions inside the channels towards the inner walls; this results in nearly empty channels and the formation of a microporous phase  $Na[ZnBP_2O_8] \cdot H_2O$  (Figure 2, right).

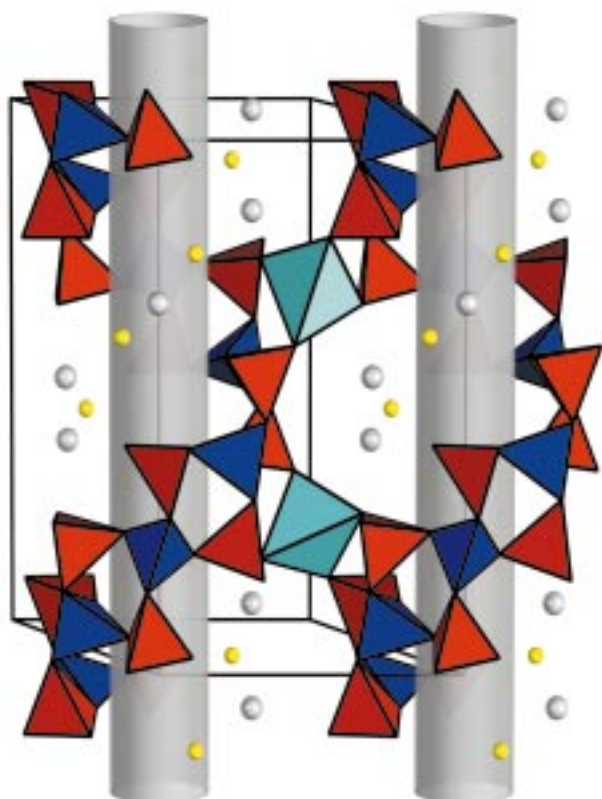


Figure 3. Linkage of borophosphate helices in the crystal structure of the dehydrated phase  $Na[ZnBP_2O_8] \cdot H_2O$  through  $ZnO_4$  tetrahedra ( $BO_4$  tetrahedra: blue,  $PO_4$  tetrahedra: red,  $Na^+$ : grey spheres,  $H_2O$  in the helical channels: yellow spheres,  $Zn^{II}$  tetrahedral: turquoise). For further details see text.

## Experimental Section

**Synthesis and analytical characterization:**  $NaZn(H_2O)_2[BP_2O_8] \cdot H_2O$  was prepared under mild hydrothermal conditions in teflon autoclaves (internal volume 20 mL). For this  $ZnCl_2$  (1.05 g),  $Na_2B_4O_7 \cdot 10H_2O$  (1.46 g), and  $Na_2HPO_4 \cdot 2H_2O$  (4.83 g) (molar ratio 2:1:7) were heated at  $80^\circ C$  in demineralized water (10 mL) and treated under stirring with 37% HCl (5 mL), until the components were completely dissolved. The clear solution was concentrated to about 12 mL by heating to give a highly viscous gel (pH 1), which then was transferred to a teflon autoclave (degree of filling about 55%) and stored at a temperature of  $170^\circ C$  for periods up to two weeks. The crystalline reaction products were separated from the mother

liquor by vacuum filtration, washed with demineralized water, and dried at  $60^\circ C$ . Single crystals (hexagonal bipyramids) were grown under these conditions to a size up to 0.6 mm. Analytical characterizations carried out by using energy dispersive X-ray analyses (SEM JEOL JSM6400, EDX-System Link ISIS300) and atomic absorption spectrometry (Perkin–Elmer AS4000) resulted in a molar ratio of sodium:zinc:boron:phosphorous of 1:1:1:2. X-ray powder investigations identified the compound to be a member of the isotypic series  $M^I M^{II}(H_2O)_2[BP_2O_8] \cdot yH_2O$  ( $M^I$ : Li, Na, K;  $M^{II}$ : Mn, Fe, Co, Ni, Zn;  $y$ : 0.5, 1).<sup>[2b, 6a]</sup>

**Thermal investigations and identification of dehydrated phases:** Difference-thermoanalytical/thermogravimetric studies on  $NaZn(H_2O)_2[BP_2O_8] \cdot H_2O$  up to temperatures of  $800^\circ C$  were carried out on a Netzsch 409TG/DTA analyzer (heating rate  $5 K min^{-1}$ , system open to air, corundum crucibles) and indicated a dehydration process running over two distinct stages. In the first step ( $105–180^\circ C$ ), two moles of  $H_2O$  per formula unit are released corresponding to a weight loss of 9.98% (calculated weight loss 10.48%). Further weight loss of 3.91% between 185 and  $347^\circ C$  is consistent with the release of most of the remaining  $H_2O$  (maximum one mole, calculated weight loss 5.24%). Powder-diffraction investigations of the reaction product after the DTA/TG experiment (maximum temperature  $800^\circ C$ ) indicated the presence of an amorphous solid.

After the first dehydration step the solid material obtained has a perfect X-ray powder pattern that could be used for a successful structure determination (see next section and Figure 5 later). The dehydrated phase  $Na[ZnBP_2O_8] \cdot H_2O$  is already (partially) rehydrated to  $NaZn(H_2O)_2[BP_2O_8] \cdot H_2O$  during cooling down inside the TA equipment (system open to air) and by keeping the TA crucible at room temperature for a period of only one hour before starting the next heating experiment. Figure 4 displays two successive DTA/TG measurements ( $T_{max} = 165^\circ C$ , heating rate  $3 K min^{-1}$ , system open to air); the first heating run (green lines) exhibits a weight loss of 9.98% (calculated 10.48%) and already shows a slight increase of weight during the cooling process. The weight loss during the second heating experiment (dashed blue line) is only 7.93%. This lower value is evidently caused by incomplete rehydration of the sample within the small TA container (only one hour at air at room temperature; small free surface area (diameter of the TA container)). A complete rehydration is obtained by exposing the powdered, dehydrated phase to moist air over a period of 12 hours (see section on “Rehydrated phase”).

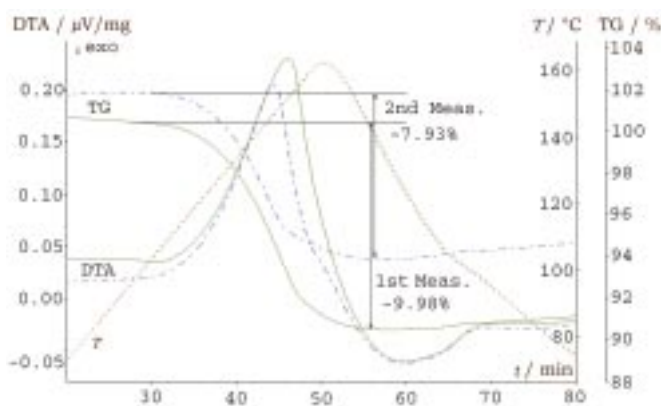


Figure 4. Two successive DTA/TG measurements (Netzsch, heating rate  $3 K min^{-1}$  (red line: temperature), system open to air,  $T_{max} = 165^\circ C$ ). First cycle (green lines), second cycle (dashed blue lines). For further details see text.

## Crystal structure determinations

**Hydrated phase—single-crystal structure analysis:** A suitable single crystal of  $NaZn(H_2O)_2[BP_2O_8] \cdot H_2O$  was investigated by taking rotation and Weissenberg photographs ( $Cu_{K\alpha}$  radiation); these showed the reflection pattern of a primitive hexagonal lattice. The interference conditions—reflections ( $000l$ ) only for  $l = 6n$ —suggested the possible space groups  $P6_1$ ,  $P6_5$ ,  $P6_22$ , and  $P6_322$ . The hexagonal unit-cell parameters were obtained on the basis of 52 centered reflections, by using the least-squares method. The reflection intensities were measured on a Siemens automated

diffractometer (graphite-monochromator, Mo<sub>Kα</sub> radiation). Details of the data collection and refinement are summarized in Table 1.<sup>[18]</sup>

The crystal structure of NaZn(H<sub>2</sub>O)<sub>2</sub>[BP<sub>2</sub>O<sub>8</sub>]·H<sub>2</sub>O was solved by direct methods which led to the positions of zinc, phosphorous, sodium, and some of the oxygen atoms. The positions of the remaining oxygen and boron atoms were derived by subsequent least-squares and difference Fourier syntheses.<sup>[19]</sup> Positional parameters and anisotropic displacement parameters were refined by full-matrix least-squares for all atoms (see Table 2).

Table 1. Crystallographic data of NaZn(H<sub>2</sub>O)<sub>2</sub>[BP<sub>2</sub>O<sub>8</sub>]·H<sub>2</sub>O.

crystal system	hexagonal
space group	<i>P</i> 6 <sub>1</sub> 22 (No. 178)
<i>a</i> [pm]	946.2(2)
<i>c</i> [pm]	1583.5(1)
cell volume [10 <sup>6</sup> pm <sup>3</sup> ]	1227.8(4)
<i>Z</i>	6
ρ <sub>calcd</sub> [g cm <sup>-3</sup> ]	2.736
crystal color, habit	colorless, hexagonal bipyramids
crystal size [mm <sup>3</sup> ]	0.30 × 0.15 × 0.15
<i>T</i> [°C]	20
μ(Mo <sub>Kα</sub> ) [mm <sup>-1</sup> ]	3.499
θ range [°]	5 ≤ 2θ ≤ 60
index range	−1 ≤ <i>h</i> ≤ 12, −13 ≤ <i>k</i> ≤ 14, −1 ≤ <i>l</i> ≤ 22
scan mode	ω
measured reflections	3217
independent reflections	1196
observed reflections [ <i>F</i> <sub>o</sub> > 4σ( <i>F</i> <sub>o</sub> )]	1020
<i>R</i> <sub>int</sub>	0.0615
corrections	Lorentzian polarization and absorption (empirical, ψ-scan)
structure solution	direct method SHELXS-86 <sup>[19]</sup>
structure refinement	SHELXL-93 <sup>[19]</sup>
parameters	75
goodness-of-fit on <i>F</i> <sup>2</sup>	1.142
Flack parameter	−0.01(3)
<i>R</i> values [ <i>F</i> <sub>o</sub> > 4σ( <i>F</i> <sub>o</sub> )]	<i>R</i> 1 = 0.0409, <i>wR</i> 2 = 0.0828
<i>R</i> values (for all data)	<i>R</i> 1 = 0.0544, <i>wR</i> 2 = 0.0905
residual electron density	0.676/−0.552
[e × 10 <sup>-6</sup> pm <sup>-3</sup> ]	

Table 2. Atomic coordinates and equivalent displacement factors [× 10<sup>4</sup> pm<sup>2</sup>] in the crystal structure of NaZn(H<sub>2</sub>O)<sub>2</sub>[BP<sub>2</sub>O<sub>8</sub>]·H<sub>2</sub>O.

	Wyckoff position	<i>x</i>	<i>y</i>	<i>z</i>	<i>U</i> <sub>eq</sub>
Na	6 <i>b</i>	0.1931(3)	0.3861(5)	0.2500	0.049(1)
Zn	6 <i>b</i>	0.54946(4)	0.09891(9)	0.2500	0.0140(2)
B	6 <i>b</i>	0.8469(4)	0.6938(9)	0.2500	0.014(1)
P	12 <i>c</i>	0.3893(1)	0.1684(1)	0.41444(8)	0.0113(2)
O1	12 <i>c</i>	0.2152(4)	0.0206(4)	0.4003(2)	0.0155(7)
O2	12 <i>c</i>	0.2935(4)	0.4908(4)	0.1124(2)	0.0190(7)
O3	12 <i>c</i>	0.3853(4)	0.3151(4)	0.3799(2)	0.0166(7)
O4	12 <i>c</i>	0.4187(4)	0.1834(4)	0.5124(2)	0.0135(6)
O5	12 <i>c</i>	0.6201(4)	0.1371(4)	0.1234(2)	0.0157(7)
O6	6 <i>a</i>	0.1340(9)	0.0000	0.0000	0.097(4)

The equivalent isotropic displacement parameter of O6<sub>H<sub>2</sub>O</sub> (located within the channels of the framework) is relatively high (0.0974). Detailed investigations carried out on a single crystal of the isotopic compound NaNi(H<sub>2</sub>O)<sub>2</sub>[BP<sub>2</sub>O<sub>8</sub>]·H<sub>2</sub>O by using polarization microscopy and X-ray single crystal investigations at low temperature (198 K) revealed no indications for twinning or disorder, because the equivalent isotropic displacement parameter of O6<sub>H<sub>2</sub>O</sub> drops significantly at lower temperature (0.063).<sup>[2b]</sup> Therefore, the relatively high equivalent isotropic displacement is to be interpreted as thermal motion of the water of crystallization O6<sub>H<sub>2</sub>O</sub>. Bond lengths and angles of the BO<sub>4</sub>, PO<sub>4</sub>, and ZnO<sub>4</sub>(H<sub>2</sub>O)<sub>2</sub> groups in the title compound are consistent with those in related borophosphates<sup>[2–8]</sup> and zinc phosphates<sup>[20]</sup> (see Table 3).

*Dehydrated phase—structure determination from X-ray powder data:* X-ray powder diffraction measurements were carried out on a Stoe Stadi-P

Table 3. Selected interatomic distances [pm] and angles [°] in the crystal structure of NaZn(H<sub>2</sub>O)<sub>2</sub>[BP<sub>2</sub>O<sub>8</sub>]·H<sub>2</sub>O.

B–O1	146.6(1) 2 ×	O1–B–O1	102.8(5)
B–O4	147.4(1) 2 ×	O1–B–O4	112.5(2) 2 ×
		O1–B–O4	113.5(2) 2 ×
		O4–B–O4	102.6(5)
P–O1	155.4(3)	O1–P–O3	105.8(2)
P–O3	151.0(3)	O1–P–O4	107.8(2)
P–O4	157.0(3)	O1–P–O5	111.1(2)
P–O5	150.4(3)	O3–P–O4	111.1(2)
		O3–P–O5	115.4(2)
		O4–P–O5	106.5(2)
Zn–O2	222.0(3) 2 ×	O2–Zn–O2	88.2(2)
Zn–O3	206.6(3) 2 ×	O2–Zn–O3	174.2(1) 2 ×
Zn–O5	208.8(3) 2 ×	O2–Zn–O3	88.1(1) 2 ×
		O2–Zn–O5	81.2(2) 2 ×
		O2–Zn–O5	86.3(2) 2 ×
		O3–Zn–O3	95.8(2)
		O3–Zn–O5	102.2(1) 2 ×
		O3–Zn–O5	89.4(1) 2 ×
		O5–Zn–O5	162.8(2)
Na–O2	238.5(4) 2 ×		
Na–O5	253.2(6) 2 ×		
Na–O6	260.0(5) 2 ×		
Na–O3	303.6(5) 2 ×		
O6...O6 <sup>[b]</sup>	293		

[a] O2: H<sub>2</sub>O-ligands of the Zn-coordination octahedra. O6: H<sub>2</sub>O molecules at the inner walls of the ∞<sup>1</sup>channels. [b] Hydrogen bond within the ∞<sup>1</sup>channels.

diffractometer with Cu<sub>Kα1</sub> radiation (λ<sub>Kα1</sub> = 154.059 pm, Ge monochromator) and a linear position-sensitive detector (PSD) in Debye-Scherrer geometry by using the capillary technique (diameter 0.1 mm). The preparation of the dehydrated phase Na[ZnBP<sub>2</sub>O<sub>8</sub>]·H<sub>2</sub>O (heat treatment of the hydrated phase at 180 °C for two hours) was carried out in a glove box under argon atmosphere. No correction for absorption has been applied to the data.

The X-ray powder data of the dehydrated phase Na[ZnBP<sub>2</sub>O<sub>8</sub>]·H<sub>2</sub>O could be indexed by using the program ITO.<sup>[21]</sup> The parameters of the primitive hexagonal lattice with *a* = 954.04(2), *c* = 1477.80(3) pm and *V* = 1164.88(5) × 10<sup>6</sup> pm<sup>3</sup> (values from final Rietveld structure refinement) led to the conclusion that the unit cell contains six formula units (assuming 12 × 10<sup>6</sup> pm<sup>3</sup> required space per non-hydrogen atom; data are summarized in Table 4). The systematic absences from the X-ray powder pattern (00*l*, *l* = 6*n*) led to the extinction symbol *P*6<sub>1</sub>, which corresponds to the possible space groups *P*6<sub>1</sub>, *P*6<sub>5</sub>, *P*6<sub>1</sub>22, and *P*6<sub>5</sub>22. A structure solution procedure was then carried out by using the program TOPAS.<sup>[22]</sup> First of all, a Pawley<sup>[23]</sup> fit without a structure model was performed for all possible space groups individually in order to get lattice and peak shape parameters for the energy-minimization/simulated-annealing calculations. The best fitting of the powder pattern was achieved in *P*6<sub>1</sub>22. With this space group a Rietveld refinement that included additional refineable functions for structure solution was carried out. By using the Lenard-Jones potential equation for the lattice energy minimization in combination with a simulated annealing process (for details of this process see<sup>[22]</sup> and references therein) a satisfying result was obtained. The energy potentials were set-up assuming mean bond lengths calculated from the single-crystal structure refinement. During the refinement, parameters for the profile, background (values from the Pawley fitting were used), site occupation, and temperature factors were fixed, while zero-point and lattice parameters were refined. As a result a minimum was found (within three hours calculation time on a PII 300 MHz Pentium PC), but still with differences between the observed and calculated intensities. Unusually small bond lengths between cation–cation and anion–anion pairs close to special crystallographic positions could be identified as atoms occupying special positions. After setting-up the right positions a Rietveld refinement was carried out without using energy-minimization/simulated-annealing equations. All positions were checked for occupation and in a final Rietveld refinement all positional and displacement parameters were refined for all atoms independently (Table 5), while hydrogen atoms of the water

Table 4. Crystallographic data of the dehydrated phase Na[ZnBP<sub>2</sub>O<sub>8</sub>]·H<sub>2</sub>O and rehydrated phase NaZn(H<sub>2</sub>O)<sub>2</sub>[BP<sub>2</sub>O<sub>8</sub>]·H<sub>2</sub>O.

	Dehydrated	Rehydrated
formula	Na[ZnBP <sub>2</sub> O <sub>8</sub> ]·H <sub>2</sub> O	NaZn(H <sub>2</sub> O) <sub>2</sub> [BP <sub>2</sub> O <sub>8</sub> ]·H <sub>2</sub> O
<i>M<sub>r</sub></i> [g mol <sup>-1</sup> ]	307.15	341.16
crystal system		hexagonal
space group		<i>P</i> 6 <sub>1</sub> 22 (no. 178)
diffractometer		Stoe STADI P
monochromator		Ge(111)
$\lambda$ [pm]		154.06
<i>T</i> [°C]		20
<i>a</i> [pm]	954.04(2)	946.395(8)
<i>c</i> [pm]	1477.80(3)	1581.68(2)
<i>V</i> [10 <sup>6</sup> pm <sup>3</sup> ]	1164.88(5)	1226.86(3)
<i>Z</i>	6	6
$\theta$ range	9° ≤ 2 $\theta$ ≤ 103.5°	9.5° ≤ 2 $\theta$ ≤ 103°
no. data points	4701	4676
no. reflections	308	325
positional parameters	19	22
profile parameters	7	7
background parameters	8	6
<i>R</i> <sub>wp</sub>	0.052	0.074
<i>R</i> <sub>exp</sub>	0.031	0.033
goodness of fit	1.70	2.24
<i>R</i> <sub>Bragg</sub>	0.064	0.069

Table 5. Atomic coordinates and isotropic displacement factors [ $\times 10^4$  pm<sup>2</sup>] in the crystal structure of the dehydrated phase Na[ZnBP<sub>2</sub>O<sub>8</sub>]·H<sub>2</sub>O.

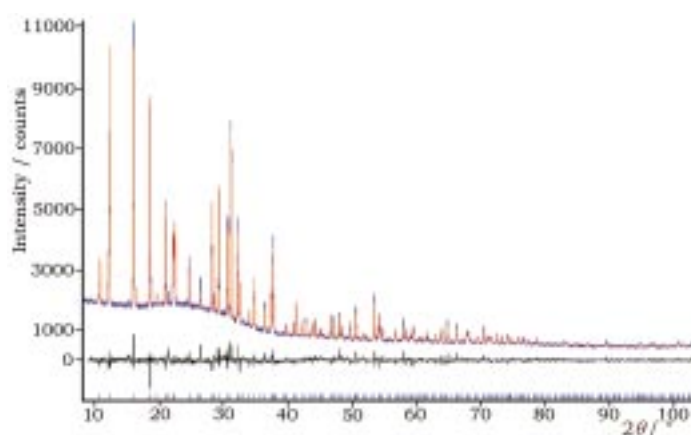
	Wyckoff position	<i>x</i>	<i>y</i>	<i>z</i>	<i>U</i> <sub>eq</sub>
Na	6 <i>b</i>	0.195(1)	0.390(1)	0.2500	0.190(5)
Zn	6 <i>b</i>	0.5149(2)	0.0298(2)	0.2500	0.009(2)
B	6 <i>b</i>	0.834(2)	0.668(2)	0.2500	0.032(9)
P	12 <i>c</i>	0.3886(6)	0.1581(6)	0.4019(3)	0.011(2)
O1	12 <i>c</i>	0.214(1)	0.011(1)	0.394(6)	0.011(3)
O3	12 <i>c</i>	0.367(1)	0.295(1)	0.3673(7)	0.022(5)
O4	12 <i>c</i>	0.444(1)	0.183(1)	0.5082(6)	0.001(1)
O5	12 <i>c</i>	0.634(1)	0.160(1)	0.1401(5)	0.024(5)
O6	6 <i>a</i>	0.238(2)	0.0000	0.0000	0.190(1)

molecules were omitted. Large values for the thermal motion were obtained for Na and O6<sub>H<sub>2</sub>O</sub> (same labelling as in the crystal structure of the hydrated phase); this was also observed in the single-crystal structure of the hydrated phase. Global *R* values, low *R*<sub>Bragg</sub> factor (Table 4), reasonable bond lengths and angles (Table 6),<sup>[16, 17, 24]</sup> and the difference plot (Figure 5)

Table 6. Selected interatomic distances [pm] and angles [°] in the crystal structure of the dehydrated phase Na[ZnBP<sub>2</sub>O<sub>8</sub>]·H<sub>2</sub>O.<sup>[a]</sup>

B–O11	154.9(3) 2 ×	O1–B–O1	93.6(3)
B–O4	149.1(3) 2 ×	O1–B–O4	114.5(4) 2 ×
		O1–B–O4	115.7(4) 2 ×
		O4–B–O4	103.3(3)
P–O1	155.2(4)	O1–P–O3	103.6(4)
P–O3	150.5(4)	O1–P–O4	109.1(4)
P–O4	163.8(4)	O1–P–O5	121.6(4)
P–O5	144.2(4)	O3–P–O4	110.3(4)
		O3–P–O5	109.9(4)
		O4–P–O5	102.3(4)
Zn–O3	196.3(3) 2 ×	O3–Zn–O3	126.6(2)
Zn–O5	201.6(3) 2 ×	O3–Zn–O5	100.5(1) 2 ×
		O3–Zn–O5	107.5(1) 2 ×
		O5–Zn–O5	115.1(2)
Na–O5	265.2(6) 2 ×		
Na–O6	209.0(5) 2 ×		
Na–O3	283.0(5) 2 ×		

[a] O6: H<sub>2</sub>O molecules at the inner walls of the  $\infty$  channels.

Figure 5. Observed (blue), calculated (red), and difference (black) X-ray powder diffraction profiles for the dehydrated phase Na[ZnBP<sub>2</sub>O<sub>8</sub>]·H<sub>2</sub>O, Cu<sub>K $\alpha$ 1</sub> radiation.

verify a successful structure determination. All other possible space groups were carefully checked and used in the same way as described, but none of them gave a sufficiently good structural model compared with the one found above.

**Rehydrated phase—structure determination from X-ray powder data:** The rehydrated phase was obtained by exposing the powdered, dehydrated compound to moist air for a period of 12 hours. The powder data of the rehydrated phase NaZn(H<sub>2</sub>O)<sub>2</sub>[BP<sub>2</sub>O<sub>8</sub>]·H<sub>2</sub>O could also be indexed by using the program ITO.<sup>[21]</sup> The parameters of the primitive hexagonal lattice with *a* = 946.395(8), *c* = 1581.68(2) pm and *V* = 1226.86(3) × 10<sup>6</sup> pm<sup>3</sup> (values from final Rietveld structure refinement) are in good agreement with the single-crystal data. The systematic absences from the X-ray powder pattern (*h*00*l*, *l* = 6*n*) led to the extinction symbol *P*6<sub>1</sub>, which corresponds to the possible space groups *P*6<sub>1</sub>, *P*6<sub>5</sub>, *P*6<sub>1</sub>22, and *P*6<sub>5</sub>22 and fits very well to the single-crystal X-ray structure data. A Rietveld refinement of the structure using the program TOPAS<sup>[22]</sup> was carried out with the space group *P*6<sub>1</sub>22, because the structure of the single crystal was solved in this space group. Moreover, the same atomic position data were used as for the starting model. Positional parameters were refined for all atoms independently (Table 7), while hydrogen atoms of the water molecules were omitted.

Table 7. Atomic coordinates and isotropic displacement factors [ $\times 10^4$  pm<sup>2</sup>] in the crystal structure of the rehydrated phase NaZn(H<sub>2</sub>O)<sub>2</sub>[BP<sub>2</sub>O<sub>8</sub>]·H<sub>2</sub>O.

	Wyckoff position	<i>x</i>	<i>y</i>	<i>z</i>	<i>U</i> <sub>eq</sub>
Na	6 <i>b</i>	0.1913(3)	0.3826(3)	0.2500	0.029(2)
Zn	6 <i>b</i>	0.5497(1)	0.0994(1)	0.2500	0.003(1)
B	6 <i>b</i>	0.8395(8)	0.6790(8)	0.2500	0.002(1)
P	12 <i>c</i>	0.3917(3)	0.1694(3)	0.4144(1)	0.002(1)
O1	12 <i>c</i>	0.2105(6)	0.01992(5)	0.3984(3)	0.005(1)
O2	12 <i>c</i>	0.2896(5)	0.4892(5)	0.1120(3)	0.010(2)
O3	12 <i>c</i>	0.3866(5)	0.3186(5)	0.3760(3)	0.005(1)
O4	12 <i>c</i>	0.4284(6)	0.1862(5)	0.5087(2)	0.005(1)
O5	12 <i>c</i>	0.6157(5)	0.1386(6)	0.1268(3)	0.005(1)
O6	6 <i>a</i>	0.1513(9)	0.0000	0.0000	0.165(1)

Isotropic displacement parameters were constrained to be equal for the tetrahedrally coordinated B and P and for the oxygen atoms labeled 1, 3, 4, and 5, while the others were refined unconstrained. This led to a very good refinement and the structural parameters were in good agreement with the X-ray single-crystal result. Global *R* values, low *R*<sub>Bragg</sub> factor (Table 4), and the difference plot (Figure 6), which shows only minor deviations, indicate a successful structure refinement. No other phases or impurities in the X-ray data could be found. Remarkably high displacement parameters again were calculated for Na and O6<sub>H<sub>2</sub>O</sub>. This has been also observed in the single-crystal investigation and accounts for only weak bonds between the

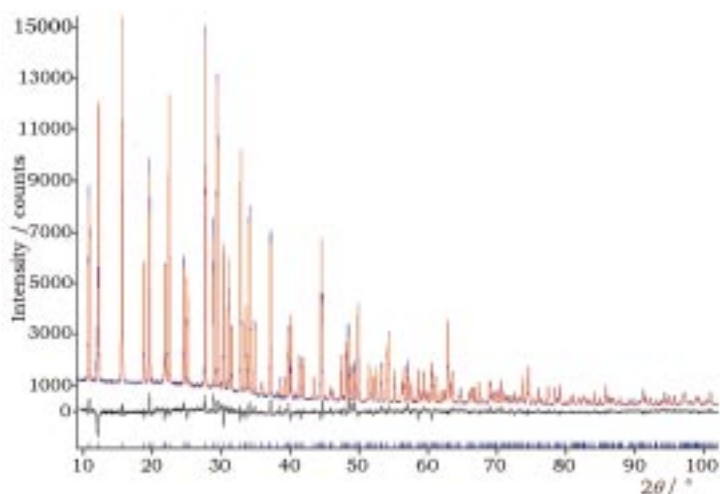


Figure 6. Observed (blue), calculated (red), and difference (black) X-ray powder diffraction profiles for the rehydrated phase  $\text{NaZn}(\text{H}_2\text{O})_2[\text{BP}_2\text{O}_8] \cdot \text{H}_2\text{O}$ ,  $\text{Cu}_{\text{K}\alpha 1}$  radiation.

coordination partners. The other possible space groups were checked in order to give a better structural model for the observed powder pattern, but these attempts failed.

### Acknowledgement

This work was supported by the Pinguin-Stiftung (Düsseldorf, Germany) and by the Fonds der Chemischen Industrie. The authors would like to thank Prof. Dr. R. A. Fischer (Ruhr-Universität Bochum, Germany) for a helpful cooperation and Dr. A. Kern (Bruker AXS GmbH Karlsruhe, Germany) for providing the TOPAS software.

- [1] A. K. Cheetham, G. Férey, T. Loiseau, *Angew. Chem.* **1999**, *111*, 3466–3492; *Angew. Chem. Int. Ed.* **1999**, *38*, 3268–3292.
- [2] a) R. Kniep, H. Engelhardt, C. Hauf, *Chem. Mater.* **1998**, *10*, 2930–2934; b) I. Boy, Ph.D. dissertation, Darmstadt University of Technology, to be found under <http://elib.tu-darmstadt.de/diss/000044/>, **1999**.
- [3] R. Kniep, G. Gözel, B. Eisenmann, C. Röhr, M. Asbrand, M. Kizilyalli, *Angew. Chem.* **1994**, *106*, 791–793; *Angew. Chem. Int. Ed. Engl.* **1994**, *33*, 749–751.
- [4] a) I. Boy, G. Cordier, R. Kniep, *Z. Kristallogr. New Cryst. Struct.* **1998**, *213*, 29–30; b) I. Boy, G. Cordier, B. Eisenmann, R. Kniep, *Z. Naturforsch. Teil B* **1998**, *53*, 165–170; c) I. Boy, G. Cordier, R. Kniep, *Z. Naturforsch. Teil B* **1998**, *53*, 1440–1444; d) C. Hauf, I. Boy, R. Kniep, *Z. Kristallogr. New Cryst. Struct.* **1999**, *214*, 3–4; e) I. Boy, G. Schäfer, R. Kniep, *Z. Anorg. Allg. Chem.*, in press.
- [5] a) C. Hauf, T. Friedrich, R. Kniep, *Z. Kristallogr.* **1995**, *210*, 446; b) C. Hauf, R. Kniep, *Z. Kristallogr.* **1996**, *211*, 705–706; c) C. Hauf, R. Kniep, *Z. Kristallogr.* **1996**, *211*, 707–708; d) C. Hauf, R. Kniep, *Z. Kristallogr. New Cryst. Struct.* **1997**, *212*, 313–314; e) I. Boy, C. Hauf, R. Kniep, *Z. Naturforsch. Teil B* **1998**, *53*, 631–633; f) R. Kniep, I. Boy, H. Engelhardt, *Z. Anorg. Allg. Chem.* **1999**, *625*, 1512–1516.
- [6] a) R. Kniep, H. G. Will, I. Boy, C. Röhr, *Angew. Chem.* **1997**, *109*, 1052–1053; *Angew. Chem. Int. Ed. Engl.* **1997**, *36*, 1013–1014; b) I. Boy, R. Kniep, *Z. Naturforsch. Teil B* **1999**, *54*, 895–898.
- [7] a) R. Kniep, H. Engelhardt, *Z. Anorg. Allg. Chem.* **1998**, *624*, 1291–1297; b) R. Kniep, G. Schäfer, *Z. Anorg. Allg. Chem.* **2000**, *626*, 141–147.
- [8] C. Hauf, R. Kniep, *Z. Naturforsch.* **1997**, *52b*, 1432–1435.
- [9] D. W. Breck, *Zeolite Molecular Sieves*, Wiley, New York, **1974**.
- [10] a) S. T. Wilson, B. M. Lok, C. A. Messina, T. R. Cannan, E. M. Flanigen, *J. Am. Chem. Soc.* **1982**, *104*, 1146–1147; b) E. M. Flanigen, B. M. Lok, R. L. Patton, S. T. Wilson, *Pure Appl. Chem.* **1986**, *58*, 1351–1358.
- [11] a) P. Feng, X. Bu, G. D. Stucky, *Nature* **1997**, *388*, 735–741; b) M. Hartmann, L. Kevan, *Chem. Rev.* **1999**, *3*, 636–663.
- [12] a) M. Estermann, L. B. McCusker, C. Baerlocher, A. Merrouche, H. Kessler, *Nature* **1991**, *352*, 320–323; b) T. Loiseau, G. Férey, *J. Solid State Chem.* **1994**, *111*, 403–415.
- [13] a) R. L. Bedard (UOP Inc. USA), US 005302362, **1994** [*Chem. Abstr.* **1994**, *121*, 208502q]; b) W. T. A. Harrison, L. Hannooman, *Angew. Chem.* **1997**, *109*, 663–665; *Angew. Chem. Int. Ed. Engl.* **1997**, *36*, 640–641; c) S. B. Harmon, S. C. Sevov, *Chem. Mater.* **1998**, *10*, 3020–3023.
- [14] a) R. Kniep, G. Schäfer, H. Engelhardt, I. Boy, *Angew. Chem.* **1999**, *111*, 3858–3861; *Angew. Chem. Int. Ed.* **1999**, *38*, 3641–3644; b) R. Kniep, G. Schäfer, H. Borrmann, *Z. Kristallogr. New Cryst. Struct.* **2000**, *215*, 335–336.
- [15] Ch. Baerlocher and L. B. McCusker, *Atlas of Zeolite Structures Types*, to be found under <http://www.iza-sc.ethz.ch/IZA-SC/Atlas/data/CZP.html>.
- [16] W. T. A. Harrison, T. E. Gier, G. D. Stucky, R. W. Broach, R. A. Bedard, *Chem. Mater.* **1996**, *8*, 145–151.
- [17] a) N. Rajic, N. Z. Logar, V. Kaucic, *Zeolites* **1995**, *15*, 672–678; b) M. Helliwell, J. R. Helliwell, V. Kaucic, N. Z. Logar, L. Barba, E. Busetto, A. Lausi, *Acta Crystallogr. Sect. B* **1999**, *55*, 327–332.
- [18] Further details on the crystal structure investigations may be obtained from the Fachinformationszentrum Karlsruhe, 76344 Eggenstein-Leopoldshafen, Germany (fax: (+49)7247-808-666; e-mail: [crysdata@fiz-karlsruhe.de](mailto:crysdata@fiz-karlsruhe.de)), on quoting the depository numbers CSD-411394, CSD-411395, and CSD-411396.
- [19] a) SHELXS-86 G. M. Sheldrick, *Acta Crystallogr. Sect. A* **1990**, *46*, 467; b) SHELXL-93 G. M. Sheldrick, Universität Göttingen, **1993**.
- [20] S. Abid, M. Rzaigui, *Eur. J. Solid State Inorg. Chem.* **1995**, *32*, 927–935.
- [21] J. W. Visser, *J. Appl. Crystallogr.* **1969**, *2*, 89–95.
- [22] A. A. Coelho, *J. Appl. Crystallogr.* **2000**, *33*, 899–908.
- [23] G. S. Pawley, *J. Appl. Crystallogr.* **1981**, *14*, 357–361.
- [24] M. T. Averbuch-Pouchot, J. C. Guitel, *Acta Crystallogr. Sect. B* **1977**, *33*, 1427–1431.

Received: July 31, 2000 [F2637]